Resonant Impurity Bands in Semiconductor Superlattices

Dominik Stehr,[1,*] Claus Metzner,[2] Manfred Helm,[1] Tomas Roch,[3] and Gottfried Strasser[3]

[1]*Institute of Ion Beam Physics and Materials Research, Forschungszentrum Rossendorf, P.O. Box 510119, 01314 Dresden, Germany*
[2]*Institut für Technische Physik I, Universität Erlangen, Erwin-Rommel-Strasse 1, 91058 Erlangen, Germany*
[3]*Institut für Festkörperelektronik, TU Wien, Floragasse 7, 1040 Wien, Austria*

(Received 3 August 2005; published 12 December 2005)

It is shown that the $2p_z$ confined impurity state of a semiconductor quantum well develops into an excited impurity band in the case of a superlattice. This is studied by following theoretically the transition from a single to a multiple quantum well or superlattice by exactly diagonalizing the three-dimensional Hamiltonian for a quantum well system with random impurities. Intersubband absorption experiments, which can be nearly perfectly reproduced by the theory, corroborate this interpretation, which also requires reinterpretation of previous data.

DOI: 10.1103/PhysRevLett.95.257401 PACS numbers: 78.67.Pt, 73.20.Hb, 73.21.Cd

Semiconductor superlattices, consisting of a periodic sequence of thin layers of different semiconductors, can serve as a model system for a wealth of phenomena in solid state physics. The artificial periodicity in one dimension (the growth direction of the epitaxial layer) allows one to create tailored band structures with so-called minibands and minigaps, which are much narrower than the bands (and gaps) in natural bulk crystals. Such structures have enabled researchers the first observation of phenomena like Bloch oscillations and Wannier-Stark ladders [1].

A fundamental problem in semiconductor physics is the existence of localized states in addition to extended band states, which are unavoidable due to disorder and doping, and give rise to a metal-insulator transition as a function of doping density [2]. In an effective-mass framework, the limit of low doping and zero compensation is equivalent to a system of isolated hydrogen atoms, resulting in the well known shallow impurity levels located below the conduction band. At higher doping densities, impurity bands are formed due to the interaction between doping atoms, and eventually the impurity band develops into a band tail of localized states. The metal-insulator transition (MIT) usually occurs while the Fermi energy is located in the impurity band [3]. In a slightly metallic semiconductor, the MIT can be induced by a magnetic field, which leads to stronger confinement of the wave functions and thus to localization [4].

Confining an impurity in a quantum well (QW) has two prime effects: (1) The binding energy is increased from one effective Rydberg (Ry*) in three dimensions up to four Ry* in the ideally two-dimensional case [5]. For a realistic QW the value is somewhere in between [6]. (2) Because of the reduced symmetry of the problem, the degeneracy of the hydrogenic states is reduced. If still the terminology of the 3D hydrogen atom is used, the $2p_z$ (or $2p_0$, where $m = 0$ is the magnetic quantum number) state is split off from the $2p_{xy}$ levels and becomes a resonant state lying just below the second ($n = 2$) quantum well subband [7,8]. In fact, this $2p_0$ level becomes the ground state of a new 2D hydrogenic series associated with the $n = 2$ subband. The exact correspondence between 3D and 2D hydrogenic states has been discussed in Ref. [9]. The $2p_0$ level has been observed in Raman scattering [10] and infrared spectroscopy [11]; in particular, the $1s$-$2p_0$ transition can be regarded as an impurity shifted intersubband transition, slightly higher in energy than the latter. In semiconductor superlattices, the $1s$-$2p_0$ transition has been very clearly revealed [12], since because of the finite miniband width it is spectrally separated from the van Hove singularities in the interminiband absorption spectra; recently it has also been observed in the infrared absorption of isolated quantum wells [13].

In this Letter we show that this picture has to be modified. We numerically calculate the energy levels of a finite quantum well system with impurities and follow the evolution from a double quantum well to a superlattice. We show that each subband level has its associated impurity level (series) attached, and in the limit of a superlattice, also the impurity levels lie dense and form a resonant impurity band, energetically overlapping the associated miniband (see Fig. 1). Energy levels and wave functions are not easily experimentally accessible in a direct manner; therefore we are calculating the infrared absorption as an observable quantity, which is compared to experimental absorption spectra. Apart from the amazing agreement, we are able to explain some hitherto not understood observations in the regime of the magnetically induced metal-

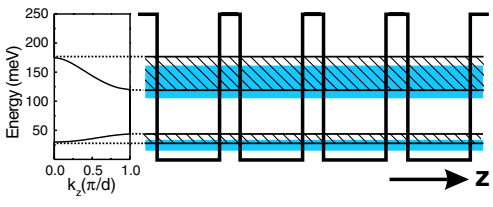

FIG. 1 (color online). Schematic of a superlattice with minibands (hatched) and impurity bands (shaded blue area), slightly lower in energy than the minibands (see later in the text).

insulator transition [14], leading to a reinterpretation of existing data.

Previous calculations of impurity levels in quantum wells were often based on variational approaches [5,8,11], and mostly low-lying levels have been investigated. Yet already in 1984 Priester *et al.* [7] showed that each 2D subband has an impurity band associated with it. Serre *et al.* [15] performed calculations of the density of states (DOS) in a multiple-scattering approach, later on also used in [16] for δ-doped layers. Other works include low-lying states in a double QW [17] and a fully numerical investigation of the DOS in a 2D system with random impurities [18].

For our calculation we start from a fully three-dimensional Hamiltonian which contains the z-dependent quantum well potential on the basis of the effective-mass approximation, the Coulomb potential of impurities at a certain location z_0, but randomly distributed in the xy plane, and the Hartree potential of the electrons in the z direction. Electron-electron interaction is neglected in this study. In this framework we solve the Schrödinger equation for N coupled quantum wells ($N = 1, \ldots, 20$) numerically exact on a square of 100×100 nm^2 with periodic boundary conditions in the xy direction. Putting one impurity into this square corresponds to a density of $n = 1 \times 10^{10}$ cm^{-2}. The method follows closely the one published in Ref. [19]. Thus, there are no *a priori* assumptions concerning the impurity states, as they are contained in any variational ansatz (which has been the main tool in the past to calculate shallow impurity levels in quantum wells [5,8,11]). Typically the calculation results in several hundred to thousands of energy levels. We calculate the optical transition matrix elements between all of them and use these together with the correct occupation via Fermi-Dirac statistics to calculate the absorption coefficient (with radiation polarized along the growth direction z). As a result, we get, for the first time to our knowledge, a QW or superlattice infrared absorption spectrum that treats subbands and impurity states on the same footing. In addition, we average the spectra over several impurity configurations and convolve them with a Lorentzian of width 4 meV. The latter accounts for homogeneous broadening and removes all fine structures resulting from the finiteness (discreteness) of the system. We are also able to identify the energy level pairs that give the strongest contribution to the absorption spectra.

We start by discussing a symmetric double quantum well. Its energy levels are grouped into doublets (Fig. 2, inset), split by the thin tunneling barrier. Note that these states can be regarded as precursors to the miniband edges in a superlattice. Figure 2 shows the results of such a calculation for a GaAs/$Al_{0.3}Ga_{0.7}$As double quantum well with a doping density of $n = 1 \times 10^{10}$ cm^{-2} in each QW (thickness of each well 9 nm, barrier thickness 2.5 nm) at temperatures 4, 50, 100, and 300 K [20]. Let us start with

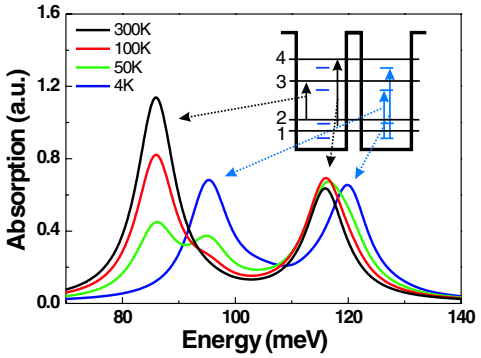

FIG. 2 (color online). Calculated infrared absorption spectra of a double quantum well for different temperatures as indicated. A sketch of the structure is shown in the inset with the relevant transitions.

the high-temperature spectra. Two absorption peaks are observed at 86 and 116 meV, corresponding to the $2 \rightarrow 3$ and $1 \rightarrow 4$ intersubband transitions, respectively (but note that, strictly, the subband index is not a good number in the presence of impurities). The former one occurs because the $n = 2$ state is thermally occupied at 300 K. The relative peak heights reflect the larger oscillator strength for the $2 \rightarrow 3$ compared to the $1 \rightarrow 4$ transition. The $1 \rightarrow 3$ and $2 \rightarrow 4$ transitions are parity forbidden in a symmetric structure. At low temperature the $2 \rightarrow 3$ peak disappears due to thermal depopulation of the $n = 2$ subband; instead a peak at 95 meV appears, which can be identified as the transition between the $1s$ impurity ground state and the $m = 0$ resonant impurity state associated with the $n = 3$ subband. Note that these spectra are already reminiscent of experimental superlattice spectra (e.g., Ref. [12]), where the $1 \rightarrow 4$ transition would correspond to the singularity at the mini-Brillouin zone center (at $k_z = 0$) and the $2 \rightarrow 3$ transition at its edge (at $k_z = \pi/d$, where d is the superlattice period).

Let us now analyze the behavior of the high-energy peak around 116 meV. As the temperature is lowered, it shifts to slightly higher energy (to 120 meV). In our model, this shift is not related to a variation of band parameters or many-body effects; hence, it must be related to single-particle energies. In fact, a closer inspection shows that at low temperature this peak can be identified with the transition from the impurity ground state to the $m = 0$ state associated with the $n = 4$ level; i.e., it is the "impurity shifted" $1 \rightarrow 4$ transition. This assignment can be proven by looking at the wave functions in the xy plane. At first we identify the energy levels that give the major contribution to the absorption spectrum, and, in particular, to the 116–120 meV peak, at high and low temperatures. Table I lists the transitions between the calculated quantum states in order of descending strength. At $T = 4$ K there are just four strong transitions, from the impurity ground states in the two QWs ($i = 0, 1$) to the excited impurity state associated with the $n = 3$ and 4 subbands, respectively [21].

TABLE I. List of the strongest transitions at $T = 4$ K (left) and $T = 300$ K (right). Listed are the initial (i) and final (j) states of each transition, their respective oscillator strengths, f_{ij}, and energies, ϵ_{ij}. The transition in last line at $T = 300$ K is the strongest around 116 meV, but totally the 23rd strongest. The wave functions of the bold states are plotted in Fig. 3.

	4 K			300 K	
$i \to j$	f_{ij}	ϵ_{ij} [meV]	$i \to j$	f_{ij}	ϵ_{ij} [meV]
$1 \to 272$	0.35	94.5	$17 \to 286$	0.022	85.95
$0 \to 275$	0.31	96.1	$33 \to 307$	0.020	85.94
$0 \to$ **391**	0.28	119.6	...	...	...
$1 \to 392$	0.27	120.6	...	...	...
$0 \to 6$	0.16	9.2	$10 \to$ **415**	0.012	115.85

The fifth-strongest transition is one in the far infrared, related to the $2p_0$ state near the $n = 2$ subband (not shown or further discussed here for simplicity). The squared modulus of the xy wave function of the state $j = 391$ (integrated over the z coordinate) is plotted in Fig. 3 (left panel). This is clearly a state that is strongly localized around the position of the impurity ions. Note that at 4 K the Fermi energy lies between the impurity ground state and the first subband; i.e., only impurity states are occupied. At $T = 300$ K the situation is completely different. There is a large number of transitions that contribute to the observed peaks, none of them with oscillator strength greater than 0.022. Looking at one of these final states ($j = 415$, the strongest one with transition energy around 116 meV, right panel of Fig. 3), it is clear that this is an extended state. The maxima and minima of the probability distribution are related to the impurity potentials, the involved k values, and the periodic boundary conditions. The initial state $i = 10$ is, of course, also extended. Thus we have shown that the high-energy peaks at 120 and 116 meV have an entirely different origin; namely, they originate from impurity and miniband states, respectively.

While this—a resonant impurity state associated with the $n = 4$ subband—may not be surprising for itself, it bears consequences for the situation in a superlattice, where it would correspond to a resonant impurity state associated with the *upper edge* of the second miniband [22].

As a good approximation for a superlattice, we performed the calculation for 20 coupled quantum wells (the same parameters as above, i.e., well width 9 nm, barrier thickness 2.5 nm). The impurities are distributed over 1 nm of the QW center with a density of $n = 1 \times 10^{10}$ cm^{-2} per QW (the binding energy varies negligibly over this 1 nm range and is very close to the bulk value). The calculated absorption spectra for different temperatures are shown in Fig. 4. For high temperatures the spectrum consists of a strong low-energy peak and a weaker one at higher energy. These are, according to well established interpretation [12], related to the van Hove singularities of the interminiband absorption at the edge ($k_z = \pi/d$) and the center ($k_z = 0$) of the mini-Brillouin zone, respectively (see Fig. 1). Upon lowering the temperature, the low-energy peak disappears due to thermal depopulation of the first miniband. What remains is a peak at 90 meV, which has previously been assigned to an impurity transition [12]. This interpretation remains valid by performing a similar analysis as for the double QW.

Let us now turn to the higher energy peak at 133 meV. As stated above, at high temperature this corresponds to the interminiband transition at $k_z = 0$. At low temperature, however, where it simply appears to become stronger, both the comparison with the double QW and the analysis of the wave functions [23] show that this is again an impurity transition, namely, from the ground state to the impurity state associated with the upper edge of the second miniband. In fact, the whole spectrum (from 90 to 133 meV) at $T = 4$ K is due to impurity transitions, and reflects a band of resonant states, partly overlapping the second miniband (see Fig. 1; these states are de facto localized, yet strictly they are resonant states that can decay into the continuum). Note that this is not an impurity band in the usual meaning (arising from interacting impurity ions), but results from the large number of QWs, just like the miniband. Hence, it cannot be decided by simply looking at the experimental spectrum whether the 133 meV

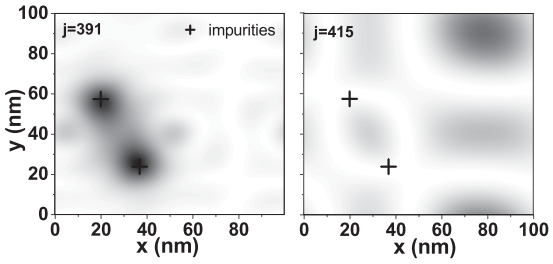

FIG. 3. Contour plot of the squared moduli of the states $j = 391$ and 415 in the xy plane (integrated over the z coordinate). The positions of the impurities (one in each QW) are indicated by crosses.

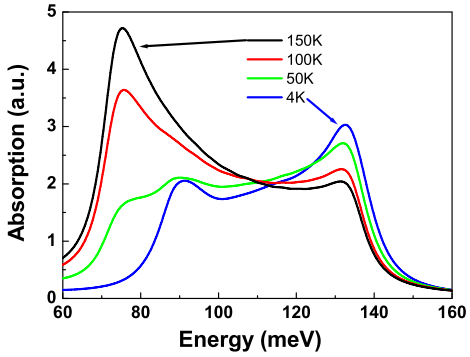

FIG. 4 (color online). Calculated infrared absorption spectra of a superlattice for different temperatures as indicated.

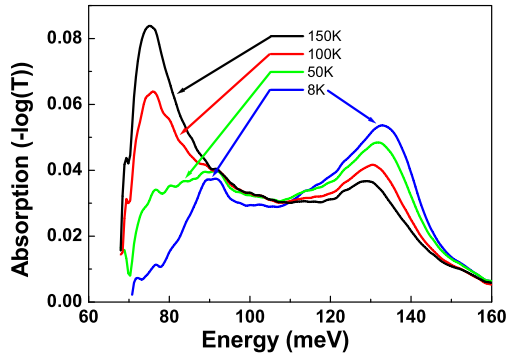

FIG. 5 (color online). Experimental infrared absorption spectrum of a $GaAs/Al_{0.3}Ga_{0.7}As$ superlattice with 9 nm well width and 2.5 nm barrier thickness. The cutoff at 70 meV is due to the detector employed in the measurement.

peak is a miniband or an impurity transition. The calculation shows that the Fermi energy at $T = 4$ K lies slightly below the bottom of the first miniband. Thus clearly, the appearance of this peak is *not* an indicator for the Fermi energy lying in the first miniband, as has been falsely assumed in the past [14]. Also, this peak will *not* disappear, when a metallic sample is driven into an insulating state via a strong magnetic field—a fact that has been observed but not understood in the past [14].

In order to demonstrate the validity of the present calculation, we have measured the interminiband absorption in a $GaAs/Al_{0.3}Ga_{0.7}As$ superlattice (well width 9 nm, barrier width 2.5 nm, 300 periods), doped with $n \approx 2 \times 10^{10}$ cm^{-2} in the center of each QW (corresponding to a bulk density of 1.7×10^{16} cm^{-3}). The sample has been prepared in a multiple-total-reflection waveguide geometry and the absorption spectra (measured in a Fourier-transform spectrometer) are obtained by normalizing the *p*-polarized signal by the *s*-polarized one. The result is displayed in Fig. 5 for different temperatures. Comparison with the theoretical spectra in Fig. 4 shows an amazing agreement of the line shapes and their temperature dependence. Low-temperature magnetotransport shows a marginally metallic behavior, with a MIT being induced by magnetic fields above 4 T. This behavior is consistent with an impurity-band metal, where the Fermi energy at low temperature lies in the impurity band [24].

In summary, we have presented a theory that is able to describe the infrared optical properties of a superlattice treating the superlattice potential and the random impurity potential in a unified framework. The occurrence of impurity bands in the continuum has been demonstrated, explaining experimentally observed spectra. By including electron-electron interaction and/or a magnetic field in the calculation, it should be possible in the future to study the metal-insulator transition as a function of doping density or induced by a magnetic field.

*Electronic address: d.stehr@fz-rossendorf.de

[1] K. Leo, *High-Field Transport in Semiconductor Superlattices* (Springer, New York, 2003).
[2] See, e.g., *Localization and Interaction in Disordered Metals and Semiconductors*, edited by D. M. Finlayson (Institute of Physics Publications, Bristol, U.K., 1986).
[3] D. Romero *et al.*, Phys. Rev. B **42**, 3179 (1990).
[4] M. C. Maliepaard *et al.*, Phys. Rev. Lett. **61**, 369 (1988).
[5] G. Bastard, Phys. Rev. B **24**, 4714 (1981); C. Mailhiot, Y.-C. Chang, and T. C. McGill, Phys. Rev. B **26**, 4449 (1982).
[6] In addition, the binding energy becomes dependent on the location with respect to the growth direction z.
[7] C. Priester, G. Allan, and M. Lannoo, Phys. Rev. B **29**, 3408 (1984).
[8] R. L. Greene and K. K. Bajaj, Phys. Rev. B **31**, 4006 (1985).
[9] J. P. Cheng and B. D. McCombe, Phys. Rev. B **42**, 7626 (1990).
[10] T. A. Perry *et al.*, Phys. Rev. Lett. **54**, 2623 (1985).
[11] M. Helm *et al.*, Phys. Rev. B **43**, 13 983 (1991).
[12] M. Helm *et al.*, Phys. Rev. B **48**, 1601 (1993); M. Helm, Semicond. Sci. Technol. **10**, 557 (1995).
[13] M. Carras *et al.*, Phys. Rev. B **70**, 233310 (2004).
[14] W. Hilber *et al.*, Phys. Rev. B **53**, 6919 (1996); M. Helm *et al.* (unpublished).
[15] J. Serre, A. Ghazali, and A. Gold, Phys. Rev. B **39**, 8499 (1989).
[16] J. Kortus and J. Monecke, Phys. Rev. B **49**, 17 216 (1994).
[17] S. T. Yen, Phys. Rev. B **68**, 165331 (2003).
[18] M. Hofmann, M. Bockstedte, and O. Pankratov, Phys. Rev. B **64**, 245321 (2001).
[19] C. Metzner, M. Hofmann, and G. H. Döhler, Phys. Rev. B **58**, 7188 (1998).
[20] Note that our calculation also yields the low-energy spectra (<10 meV) due to impurity and intersubband transitions near the first doublet. They are not shown here since we concentrate on the comparison to midinfrared absorption experiments.
[21] Note the different level numbering: n counts the few subbands due to the z confinement, whereas i counts the levels of the full 3D calculation.
[22] In a completely different context localized states near the upper minband edge have been predicted; see H. A. Fertig and S. Das Sarma, Phys. Rev. B **42**, 1448 (1990).
[23] We suppress any detailed discussion as for the double QW, due to the large number of energy levels involved here.
[24] S. Liu *et al.*, Phys. Rev. B **45**, 1155 (1992).